Anal Bioanal Chem (2015) 407:8803–8812
DOI 10.1007/s00216-015-9039-x

RESEARCH PAPER

A newly developed molecularly imprinted polymer on the surface of TiO_2 for selective extraction of triazine herbicides residues in maize, water, and soil

Hao Ran Geng[1] · **Shan Shan Miao**[1,2] · **She Feng Jin**[1] · **Hong Yang**[1]

Received: 23 June 2015 / Revised: 23 August 2015 / Accepted: 10 September 2015 / Published online: 26 September 2015

Abstract A new surface molecularly imprinted polymer (MIP) based on nano-TiO_2 was developed using propazine (Pro) as a template molecule, ethyleneglycol dimethacrylate (EGDMA) as a crosslinker, methacrylic acid (MAA) as a functional monomer, and 2,2′-azobis (isobutyronitrile) (AIBN) as an initiator. Structures of the newly synthesized surface MIPs were characterized by Fourier transmission infrared spectrometry (FT-IR), scanning electron microscope (SEM), transmission electron microscope (TEM), and X-ray diffraction (XRD). The MIP had a good adsorption capacity and high recognition selectivity to propazine. Meanwhile, it exhibited a cross-selectivity for simazine (Sim) and atrazine (Atr). The MIPs were used as a solid phase extraction (SPE) material. Concomitant extraction, purification, and determination of three pesticides (Pro, Sim, and Atr) residues in water, soil, and maize plant and grain samples were performed by MIP-SPE coupled with high performance liquid chromatography (HPLC). The highly selective separation and enrichment of Pro, Atr, and Sim from the complex environmental media can be achieved. Thus, the newly developed technique provides an analytical platform to quantify the trace amount of Pro, Sim, and Atr residues in multi environmental media and food source.

Keywords Molecularly imprinted polymer · Propazine · Nano-TiO_2 · SPE · Environmental monitoring · Herbicide

Hao Ran Geng and Shan Shan Miao contributed equally to this work.

Electronic supplementary material The online version of this article (doi:10.1007/s00216-015-9039-x) contains supplementary material, which is available to authorized users.

✉ Hong Yang
hongyang@njau.edu.cn

[1] Jiangsu Key Laboratory of Pesticide Science, College of Science, Nanjing Agricultural University, Nanjing 210095, China

[2] Key Laboratory of Monitoring and Management of Crop Diseases and Pest Insects, Ministry of Agriculture, Nanjing Agricultural University, Nanjing 210095, China

Introduction

Triazine is a class of pre- and post-emergent herbicides used in farmland to control broadleaf weed growth for cereal production [1]. While application of triazine in agriculture has made great improvement in crop production, triazine brings about intensive contamination to crops and their surrounding environments [2]. Unlike other toxic chemicals, triazine is easy to accumulate in crops. Crop contamination with triazine not only affects the quality of cereals but also serves as a food chain pollutant, threatening human health [3, 4]. As a result, triazine has become a widespread environmental problem. Therefore, establishing a rapid and efficient analytical method to monitor triazine residues in environments and agriculture products is of particular importance [5–7].

Recently, several sample pretreatment methods have been developed for extraction and enrichment of triazine pesticides such as liquid-liquid extraction [8] and solid phase extraction (SPE) [9, 10]. However, these methods have drawbacks such as low selectivity, time-consuming process, analyte loss, and impurity introduction. Recently, molecular imprinting has become a powerful technique for preparing polymer containing recognition sites in a stable polymer matrix with the presence of desired template molecules [11–14]. The synthetic methods of molecularly imprinted polymer (MIP) include bulk polymerization, suspension polymerization, and precipitation polymerization. There are numerous template molecule

imprinted caves within MIP. The imprinted caves highly match the template in size, shape, functionality, and spatial arrangement and can rebind the target molecules with high selectivity and affinity [15, 16]. The stability, low cost, high selectivity, and ease for preparation of MIPs [17] have made MIPs attractive in analyzing drugs [18, 19], pesticides [11, 20–24], cholesterol [25], proteins [26], and peptides [27]. However, there are still some disadvantages for the conventionally made MIPs, like irregular materials shape, slow mass transfer, incomplete template removal, and low affinity, which reduce the selectivity of MIP for analytes [11, 23, 28]. Comparatively, the surface imprinting technique on nanomaterials should be superior for designing a novel procedure enabling the recognition sites at the supported material surface [11, 13, 20, 23, 28].

There are reports indicating the surface MIPs prepared by silica [29], magnetic Fe_3O_4 particles [30], graphene [31], carbon nanotubes [32], and nano-TiO_2 [27] as supporting matrix. Of these, nano-TiO_2 has excellent properties including low cost, non-toxicity, chemical and photo stability, and highly efficient photocatalytic effect [33]. In this study, we developed a new method to synthesize the molecular imprinted polymers on the surface of nano-TiO_2 using the herbicide propazine, one type of triazine family, as template molecule. Interactions between methacrylic acid (MAA) and propazine were confirmed by molecular simulation. The structure of MIPs was characterized. MIPs were evaluated through a series of binding experiments. The difference between MIP-SPE and C_{18}-SPE in separation and cencontration of triazine herbicides (propazine (Pro), simazine (Sim), and atrazine (Atr)) were investigated. Pro, Sim, and Atr in water, soil, and maize plant and grain were quantified by developed MIP-SPE-high performance liquid chromatography (HPLC). Thus, the main goal of this study was to provide an efficient, selective, and accurate method that allowed analysis on the trace triazine in multiple media.

Materials and methods

Chemicals and materials

Pesticides Sim, Atr, and Pro were provided by the Academy of Agricultural Science in Jiangsu, China, with purity of 97, 97.6, and 97 %, respectively. Acetanilide (Ace) was prepared in laboratory with purity of 98.5 %. (3-Aminopropyl) triethoxysilane and acryloyl chloride were purchased from Aladdin Co., Ltd. Ethyleneglycol dimethacrylate (EGDMA) was purchased from Shanghai Jiachen Chemical Co., Ltd. MAA was purchased from Sinopharm Chemical Co., Ltd. 2, 2′-Azobis(isobutyronitrile) (AIBN) was purchased from Tianjin Guangfu Fine Chemical Research Institute. All other chemicals were obtained from Nanjing Chemical Reagent Co., Ltd. Nano-TiO_2 (P25) was provided by Shanghai Haiyi Scientific & Trading Co., Ltd. Nano-TiO_2 was activated by heating at 100 °C for 12 h, soaked with 3.0 M HNO_3 at 25 °C for 12 h, and filtered. The TiO_2 particle was washed with double-distilled water and methanol to neutrality and dried under vacuum at 60 °C for 8 h.

Pesticide-free soil was collected from the surface layer at the Experimental Station of Nanjing Agricultural University, Nanjing. The soil was air-dried, crumbled, and sieved through a 2-mm sieve mesh. Uncontaminated maize grain were purchased from Academy of Agricultural Science in Jiangsu and cultivated under laboratory conditions. Briefly, maize seeds were surface-sterilized in a 5 % sodium hypochlorite and germinated. After 24 h, uniformly germinated seeds (10 plants per pot) were transferred to a plastic pot (1 L) containing 1120 g prepared soil, in which the concentration of Pro, Sim, and Atr were 4.35 μmol kg^{-1}. Seedlings were grown in a growth chamber under a light intensity of 300 μmol m^{-2} s^{-1} with a light/dark cycle of 14/10 h at 25/20 °C and watered to keep 70 % relative water content in soils [34]. All experiments in the study were independently performed in triplicate.

Preparation of molecular imprinting polymers

Synthesis of (3-aminopropyl) triethoxysilane-TiO_2 (APTS-TiO_2)

Aminopropyl modification of nano-TiO_2 was carried out with APTS, according to the method of Gao et al. [35] with slightly modification (Electronic Supplementary Material (ESM) Fig. S1). Briefly, 6.0 g of activated TiO_2 nanoparticles was added into anhydrous toluene to make 90 mL of mixture solution. APTS (12 mL) and moderate amounts of pyridine were added to the above solution drop by drop. The mixture was stirred under a nitrogen atmosphere at 110 °C for 24 h. The product (APTS-TiO_2) was filtered and obtained by washing several times with anhydrous toluene, acetone, ether, and methanol successively. Finally, the APTS-TiO_2 was dried under vacuum at 80 °C.

Synthesis of acrylamide-APTS-TiO_2 (AA-APTS-TiO_2)

APTS-TiO_2 (6.0 g) was added to a three-necked flask containing 120 mL anhydrous toluene. The mixture was stirred under a nitrogen atmosphere at 25 °C for 10 min. Acryloyl chloride (6 mL) and triethylamine (12.5 mL) were added into the above mixture separately. The mixture was vigorously stirred at 25 °C for 24 h under dry nitrogen. The product AA-APTS-TiO_2 was separated by centrifuge and washed several times with toluene, acetone, ether, and methanol, in that order. Finally, the AA-APTS-TiO_2 was dried under vacuum at 80 °C.

Imprinting of the propazine molecules at the surface of AA-APTS-TiO_2

MAA and EGDMA were used as the functional monomer and cross-linking agent of the imprinting polymerization, respectively. Typically, AA-APTS-TiO_2 (0.5 mg) was dispersed in 50 mL anhydrous toluene by ultrasonic vibration. MAA (210.8 mg, 2.45 mM), EGDMA (2427.18 mg, 12.25 mM), AIBN (30 mg), and propazine (142 mg, 0.62 mM) were then dissolved into the above solution. This mixing solution was purged with nitrogen for 30 min. A two-step temperature polymerization reaction was carried out in a water bath with a rate of 300 rpm. The prepolymerization was first done at 50 °C for 6 h. The final polymerization was completed at 60 °C for 12 h. The products were further aged at 85 °C for 6 h for high cross-linking density. The resultant MIP was separated from the mixed solution by centrifugation, and washed with toluene, acetone, ether, and methanol, respectively. To remove the residual template propazine, the MIP was washed with the mixed solution of methanol and acetic acid (7:1 *v*/*v*) in a Soxhlet extraction apparatus. At last, the MIP was dried under vacuum at 80 °C. Non-imprinted polymer (NIP) was prepared in the same way except for the absence of template propazine.

Molecular simulation

Simulation of interactions between template propazine and functional monomer MAA was performed using Hyperchem 7.5 software package (Hypercube, Inc., USA). All chemical structures were drawn using Chembiodraw Ultra 12.0 software. The three-dimensional structure of propazine and MAA were optimized using Molecular Mechanics Methods.The minimum energies of the structures were calculated through semiempirical quantum methods (PM3) and analyzed iteratively until the convergence value was less than 0.01 kcal mol^{-1}. The binding energy (ΔE) between template propazine and functional monomer MAA was calculated using the Eq. (1):

$$\Delta E = E_{\text{complex}} - \left(E_{\text{template}} + E_{\text{monomer}}\right) \quad (1)$$

Analysis of MIP structure

TENSOR-27 Fourier transform infrared (FT-IR) spectrometer (Bruker, Germany) with a 2 cm^{-1} resolution and a spectral range of 4000–450 cm^{-1} was employed to examine FT-IR spectra of samples by a pressed tablet (sample/KBr=1:200, *w*/*w*). An S-4800 field emission scanning electron microscope (SEM, Hitachi High-Technologies Corporation, Japan) and a Tecnai 12 transmission electron microscope (TEM, Philips, Holland) were used to monitor the size and morphology of samples. Phase identification was performed by X-ray polycrystal diffraction (XRD, Bruker-AXS Corporation, Germany) patterns, using a D8 Advance X-ray diffractometer with Cu $K_{\alpha 1}$ irradiation at γ=0.15418 nm.

Adsorption experiment

Experiments of adsorption isotherms and adsorption dynamics

MIP or NIP (5.0 mg) was added to the centrifuge tubes containing 5 mL water solution with propazine concentration varying from 0.2 to 11 mg L^{-1}. After shaken at room temperature at 100 rpm for 24 h, the mixture was centrifuged at 12,000×*g* for 5 min. The propazine concentration in the supernatant was measured by HPLC. Each experiment was conducted in triplicate. The equilibrium adsorption amount of propazine bound to the polymer was calculated according to Eq. (2):

$$Q_e = \frac{V(C_0 - C_e)}{m} \quad (2)$$

Where Q_e (mg g^{-1}) is the adsorption amount; V (mL) is the volume of the propazine solution; m (mg) is the weight of the polymer particles; C_0 and C_e are the initial and final propazine concentration in solution.

MIP or NIP (5.0 mg^{-1}) was added to 5 mL water solutions with 10 mg L^{-1} propazine. The mixtures were shaken at room temperature and 100 rpm at a regular time interval (1/6, 1/3, 1/2, 2/3, 5/6, 1, 2, 3, 4, 5, 6, 12, 18, and 24 h, respectively). The supernatant was determined by HPLC after centrifuged for 5 min. Each sample at the time interval was performed in triplicate. The equilibrium adsorption amount (Q_e) of propazine bound to the polymer was calculated according to Eq. (2).

Selective adsorption experiment

Sim, Atr, and Ace were selected for evaluating the specific recognition ability of MIP for Pro. The polymer particles (MIP or NIP) (5.0 mg) were mixed with 5 mL water solution containing the four compounds (each 0.03 mmol L^{-1}). Additionally, complex solutions with five different concentrations of four compounds were separately prepared. The concentration of Pro remained 0.03 mmol L^{-1} and the other three were 0.01–0.05 mmol L^{-1} in each complex solution. The concentration ratios of Sim, Atr, and Ace to Pro were 1/3, 2/3, 3/3, 4/3, and 5/3, respectively. MIP (5.0 mg) was mixed with 5 mL water solution with different concentrations of four compounds. All mixtures were shaken for 24 h at room temperature and centrifuged at 12,000×*g* for 5 min. The supernatants were determined by HPLC. Each experiment was repeated three times. The equilibrium

adsorption amount of substrates bound to the polymer was calculated according to Eq. (3):

$$Q_e = \frac{MV(C_0 - C_e)}{m} \quad (3)$$

Where M (g mol^{-1}) is the molar mass of the template, and the other parameters are same with Eq. (2).

Preparation and appliance of MIP-SPE cartridge

The SPE cartridge of molecularly imprinted polymers (MIP-SPE) was prepared using 3 mL empty cartridge packed with 200 mg MIP particles. The SPE cartridge was capped with PTFE frits at the top and bottom, respectively. The MIP-SPE cartridge was washed with 10 mL of methanol-acetic acid (7:1, *v*/*v*) to remove residue and preconditioned with 5 mL of methanol and 5 mL of ultrapure water. The MISPE column was attached to a vacuum manifold apparatus for analysis of environment samples. For comparison, the C_{18} column (SUPELCO, 3 mL, 500 mg) was used with a similar protocol to that of the MIP-SPE column.

The water sample (20 mL) was loaded onto the preconditioned MIP-SPE cartridge at a speed of 0.5 mL min^{-1}. The negative pressure was maintained for 10 min to remove remaining water on column. The MIP-SPE cartridge was washed with 2 mL methanol/deionized water (1:4, *v*/*v*) to purify. The eluate was removed. The cartridge was washed with 2 mL methanol and the washing methanol was collected for HPLC analysis. Each experiment was repeated in triplicate.

Dried soil (10.0 g) was extracted ultrasonically with 30 mL of acetone-water (3:1, *v*/*v*) for 30 min and centrifuged. The extraction procedure was repeated in triplicate. The extraction solution was filtered into a flask and concentrated to remove acetone at 40 °C by a rotary evaporator. The residue water was loaded onto the preconditioned MIP-SPE column at a speed of 0.5 mL min^{-1} and the eluate was discarded. The procedures of purification and analysis were the same as water sample.

Maize plant was cultivated under laboratory conditions using the methods indicated above. The maize plant and maize grains were rinded in a grinder (FW177, Taisite Instrument Co. Ltd., China). Ground maize plant (1.0 g) and maize grain (1.0 g) were extracted ultrasonically with petroleum ether and dichloromethane with 20 mL for 30 min, respectively. The extraction procedure was repeated in triplicate. The extraction solutions were concentrated to dry at 45 °C by a rotary evaporator. The residue was redissolved with 0.5 mL methanol and diluted with 30 mL distilled water. The mixture was loaded onto the preconditioned MIP-SPE column. The procedures of purification and analysis were the same as water sample. Each experiment was repeated three times.

To evaluate accuracy of the method, the spiked recoveries of samples were investigated. Water (20 mL) and soil (10.0 g) samples were prepared using an appropriate volume of standard mixture solution (Sim, Atr, and Pro) to obtain the final concentrations of 0.1, 1, and 2 μmol kg^{-1}, respectively. The maize grain and maize plant samples were spiked with each herbicide at the concentrations of 0.4, 0.8, and 2 μmol kg^{-1}, respectively. The spiked samples were incubated and left to stand for about an hour. Extraction, purification, and concentration were performed in the same way indicated above.

Propazine detection

Concentrations of propazine, Ace, Sim, Atr, and Pro in the mixture were determined by HPLC (Waters 2489, Waters Technologies Co. Ltd. USA), equipped with a 515 pump and a UV–vis detector. The C_8 column (250×4.6 mm i.d., 5 μm) was used with a mobile phase of methanol/water (65:35, *v*/*v*), detection at 230 nm, and a flow rate of 0.6 mL min^{-1}. The injection volume was 20 μL.

Results and discussion

Preparation of MIP at surface of AA-APTS-TiO_2

TiO_2 has been of considerable interest because it serves as a basis of important materials. The ability to functionalize TiO_2 may help our understanding of its fundamental properties and enhancing its performance in currently existing applications. Coating the surface of TiO_2 with functional polymers is a common way through the chemical immobilization of azo-initiators/chain-transfer agents, followed by initiating a polymerization reaction of organic monomers [35]. It was illustrated for the major steps involved in the imprinting synthesis at the surface of TiO_2 (ESM Fig. S1). In the first step, TiO_2 was chemically modified with APTS. The resultant APTS-TiO_2 was further acryloylated with acryloyl chloride (CH_2=CHCOCl) by catalysis of triethylamine in anhydrous toluene solvent, leading to the formation of AA-APTS monolayer at the surface of TiO_2. The AA-APTS-TiO_2 was then suspended in the anhydrous toluene solution containing MAA, EGDMA, propazine, and AIBN. The copolymerization of AA-APTS monolayer with MAA monomers directed the selective occurrence of imprinting polymerization at the surface of TiO_2, leading to the formation of uniform MIP.

Interaction between template and function monomers

In order to develop the specific recognition ability of MIP for propazine, interactions between the functional monomer (MAA) and template (Pro) were investigated using a molecular simulation technique at the molecular level. The lowest

energy of MAA and Pro calculated by molecular simulation were −1197.826 and −2967.5034 kcal mol^{-1}, respectively (Fig. 1A, B). Two kinds of nitrogen atoms in Pro structure could be the proton receptor with the charge of −0.205 and −0.265, respectively. The charges of hydrogen atom on the carboxyl group of MAA and the hydrogen atom on the amino group of Pro were 0.229 and 0.083, respectively, indicating that they could be the proton donor for the formation of hydrogen bonds. By calculation using Eq. (1), the energy of Pro-MAA complex and the binding energy ΔE turned out to be −4172.7616 and −7.4322 kcal mol^{-1} when Pro interacted with MAA as a mole ratio of 1:1 (Fig. 1C). The energy of Pro-MAA complex and the binding energy ΔE were −5378.1035 and −14.9481 kcal mol^{-1} when Pro interacted with MAA as a mole ratio of 1:2 (Fig. 1D). Since the lower binding energy resulted in the more stable complex, theoretic ratio between Pro and MAA was 1:2, which was consistent with the previous study [36]. In addition, the choice of the most appropriate ratio between Pro and MAA was subject to experimental approaches. Since the association between the monomer and template is governed by an equilibrium in the noncovalent approach (hydrogen-bonding in this paper), the functional monomers normally have to be added in excess relative to the number of moles of the template to favor the formation of the template–monomer complex. Therefore, the working molar ratio of Pro to MAA was 1:4, similar to previous report [37].

Characterization of MIP structures

To confirm the modification on the surface of TiO_2 and preparation of MIP, the SEM microphotographs of TiO_2, AA-APTS-TiO_2, NIP, and MIP were prepared. TiO_2 displayed an irregular surface (Fig. 2A). After the TiO_2 were modified by binding to APTS and acryloyl chloride, no significant change was observed compared with the TiO_2 (Fig. 2B). This may be the result that the modified molecule was too small. Compared with the SEM microphotographs of NIP (Fig. 2C), the MIP surface had a three-dimensional structure and appeared more porous (Fig. 2D–F), indicating that Pro was fixed with MAA at the surface of AA-APTS-TiO_2 in the presence of the cross-linker, porogen, and initiator in the polymerization system. The three-dimensional structure of MIP could be beneficial to rebind and release the template. TEM images showed that the size of TiO_2 particles was around 21 nm with an irregular shape (Fig. 2G). The diameter of spherical AA-APTS-TiO_2, which was modified using APTS and acryloyl chloride on TiO_2 successively, was about 25 nm (Fig. 2H). The uniform shell MIP with a polymer layer (about 25–37 nm thickness) was successfully synthesized (Fig. 2I, J), and the highly spherical morphology further suggest that the imprinted shells resulted from the highly selective polymerization of monomers at the surface of TiO_2.

The XRD patterns for TiO_2, NIP, AA-APTS-TiO_2, and MIP were presented in Fig. 3A. In the 2θ range of 20–80°, six characteristic peaks (25.37°, 37.85°, 48.02°, 54.03°, 55.16°, and 62.81°) indexed to TiO_2 were also well observed in NIP, AA-APTS-TiO_2, and MIP. All samples with specific diffraction peaks were highly crystallized materials. The four particles contain TiO_2 with an analase structure. The peak positions of the four samples remained unchanged, indicating that the step-by-step procedure of coating and polymerization made no crystalline structure change of TiO_2 [38, 39].

In FT-IR spectra, peaks at 3300 and 1635 cm^{-1} were attributed to the stretching vibration of hydroxyl group (Fig. 3B-TiO_2). Compared with the FT-IR of TiO_2, the peaks at 1089.67 and 1118 cm^{-1} were corresponding to the stretching vibrations of Ti–O and Ti–O–C, and the peak at 1563 cm^{-1} was pointing to N-H, indicating the modification of APTS on surface of TiO_2 (Fig. 3B-APTS-TiO_2). The peak at 1650 cm^{-1}

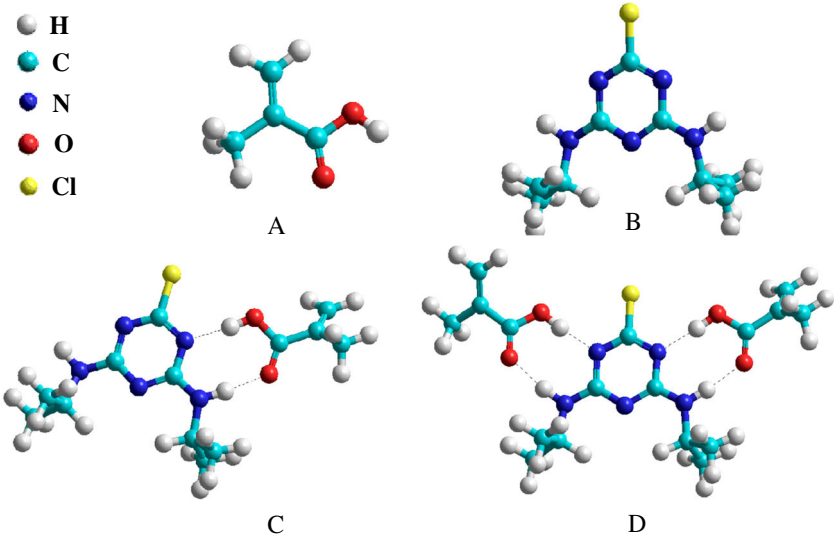

Fig. 1 Molecular simulation of interactions between propazine (Pro) and MAA. **A** MAA; **B** propazine; **C** propazine and MAA (1:1) interaction; **D** propazine and MAA (1:2) interaction

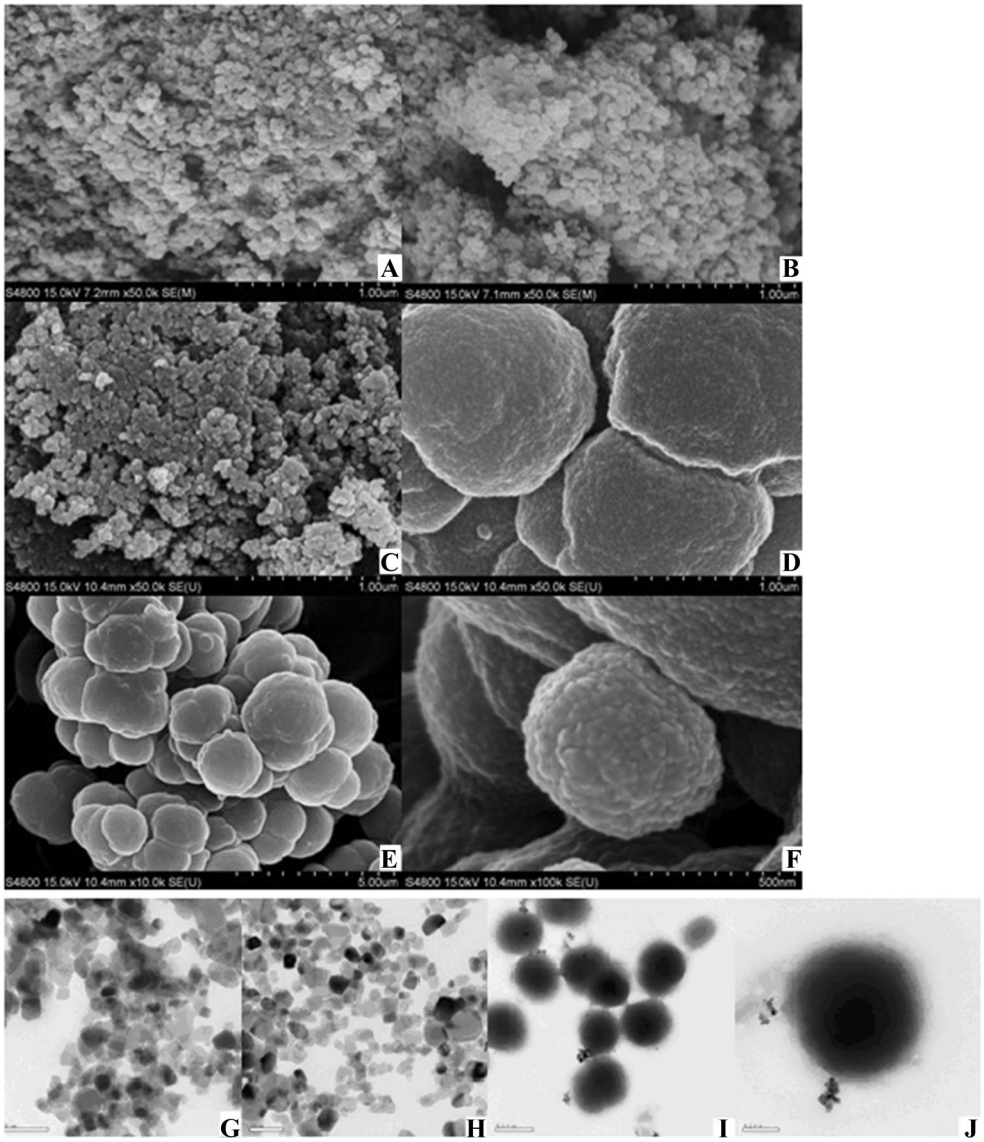

Fig. 2 The SEM (**A**–**F**) and TEM (**G**–**J**) microphotographs of MIP and NIP. **A** TiO2 (×50 k); **B** AA-APTS-TiO2 (×50 k); **C** NIP (×50 k); **D** MIP (×50 k); **E** MIP (×10 k); **F** MIP(×100 k); **G** TiO2 (50 nm); **H** AA-APTS-TiO2 (50 nm); **I** MIP (0.5 μm); **J** MIP (0.2 μm)

represented the stretching vibrations of carbonyl group in –NH-CO- group, pointing out that amination between acryloyl chloride and APTS-TiO_2 was successfully formed (Fig. 3B-AA-APTS-TiO_2). Following AA-APTS-TiO_2 reacted with EGDMA and MAA, a new peak at 1718 cm^{-1} appeared. This should be the carbonyl groups of the functional monomer MAA. Several peaks at 2950, 1454, and 1387 cm^{-1} should be attributed to CH_2 and CH_3 groups (Fig. 3B-MIP), implying that MIP was successfully prepared.

Adsorption performance of MIP

Adsorption isotherm

The binding capacity of propazine on MIP was an important parameter to estimate how much MIP was required to bind a specific amount of propazine from solution. For this purpose, the adsorption isotherm experiments were performed with initial propazine concentrations ranging from 0.2 to 11 mg L^{-1}. The adsorption amount of MIP toward propazine increased progressively with the increment of propazine, resulting from the tailor-made recognition cavities during the imprinting process (Fig. 4A). The adsorption amount of MIP (6.8076 mg g^{-1}) was 16.04-fold over that of NIP (0.4243 mg g^{-1}) when the propazine concentration was 11 mg L^{-1} (Fig. 4A). The result confirmed that the arrangement of MAA in MIP was inherently different from that of NIP. However, as the water solubility of propazine was very low, a higher concentration of propazine than 11 mg L^{-1} in water solution could not be prepared and the adsorption of MIP did not reach the saturating point even at 11 mg L^{-1} of propazine.

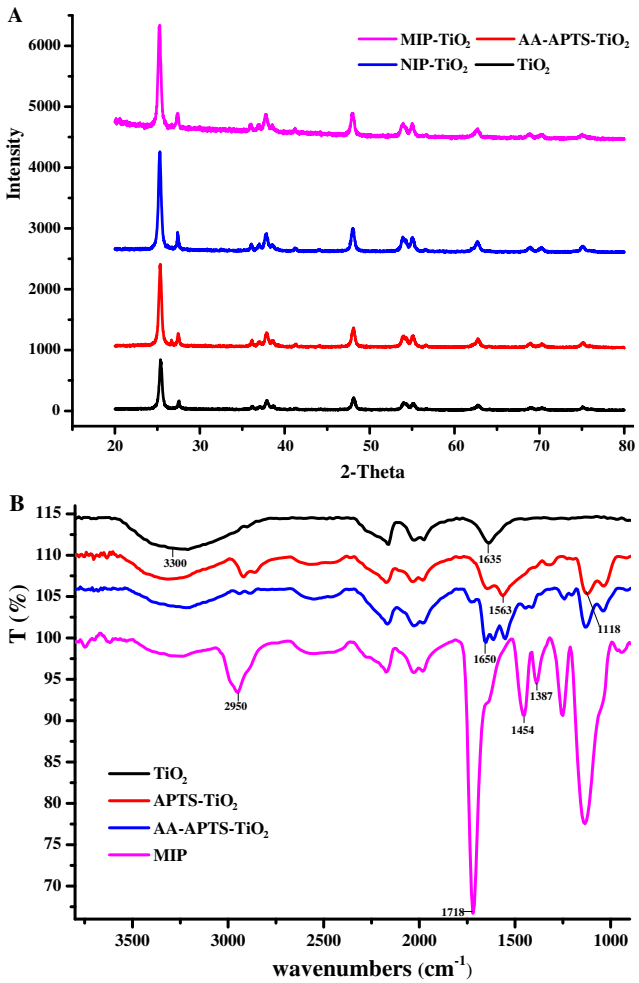

Fig. 3 XRD (**A**) of the TiO2, AA-APTS-TiO2, MIP, and NIP and FT-IR spectra (**B**) of TiO2, APTS-TiO2, AA-APTS-TiO2, and MIP

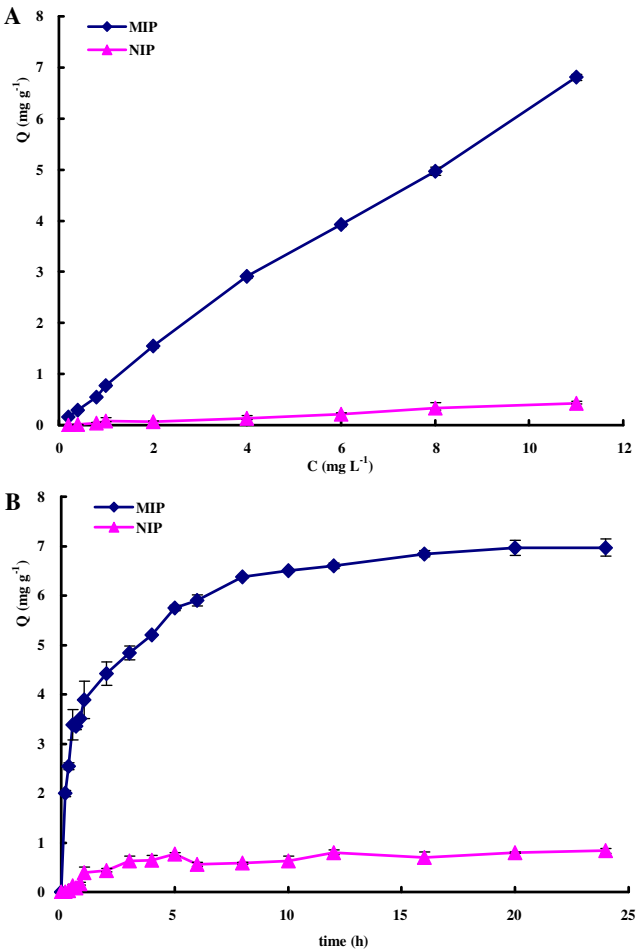

Fig. 4 Binding isotherms (**A**) of Pro on MIP and NIP. Experiment conditions: 5 mL water solution of propazine at the concentration of 0.2–11 mg L^{-1} with 5.0 mg of MIP or NIP. Adsorption dynamics (**B**) of Pro on MIP and NIP. Experiment conditions: 5 mL water solution of propazine at the concentration of 10 mg L^{-1} with 5.0 mg of MIP or NIP

Adsorption kinetic

The binding kinetics of the template propazine with MIP and NIP were also evaluated at 10 mg L^{-1} propazine. The adsorption capacity of MIP was about 8.34-fold over that of NIP during a 24-h adsorption experiment (Fig. 4B). Before the adsorption equilibrium was reached, MIP could bind propazine molecules from the solution phase at a much faster rate than the polymer NIP. MIP attained 90 % of equilibrium absorption after the first 8 h and reached the adsorption equilibrium after 15 h, whereas the NIP adsorption amount for propazine did not change obviously over time. Thus, the adsorption process could be divided into two phases: the rapid adsorption in the first 8 h and slow adsorption thereafter. Since most of the template could be access to imprinted site at a fast rate, the binding sites of MIP were suggested at the surface or in the proximity of the surface. Taken together, the high binding capablity and fast kinetic adsorption made MIP a favorable material of SPE in the pretreatment of environmental samples.

Adsorption selectivity

To investigate the selectivity of MIP for triazine herbicides, adsorption experiment was conducted using Atr and Sim as structural analogues of template propazine and Ace as a representative of different classes of compounds of dissimilar structure. NIP was used for comparison. The binding amount of propazine for MIP was higher than those of the two other triazine herbicides and acetanilide where the concentration of each compound was 0.03 mM (Fig. 5A). This suggested that the template molecule propazine had a relatively higher affinity for the imprinted polymer than others. It may be the result that the specific sites existing in MIP were complementary in shape, size, and spatial distribution to template propazine (Fig. 5A). Hydrogen bonding was formed between MAA and the hydrogen atom on the amino group and nitrogen atom of triazine ring in propazine (ESM Fig. S1). As the molecular structures of Sim and Atr were different from those of Pro in substituted group of amino group (ESM Fig. S2), the binding

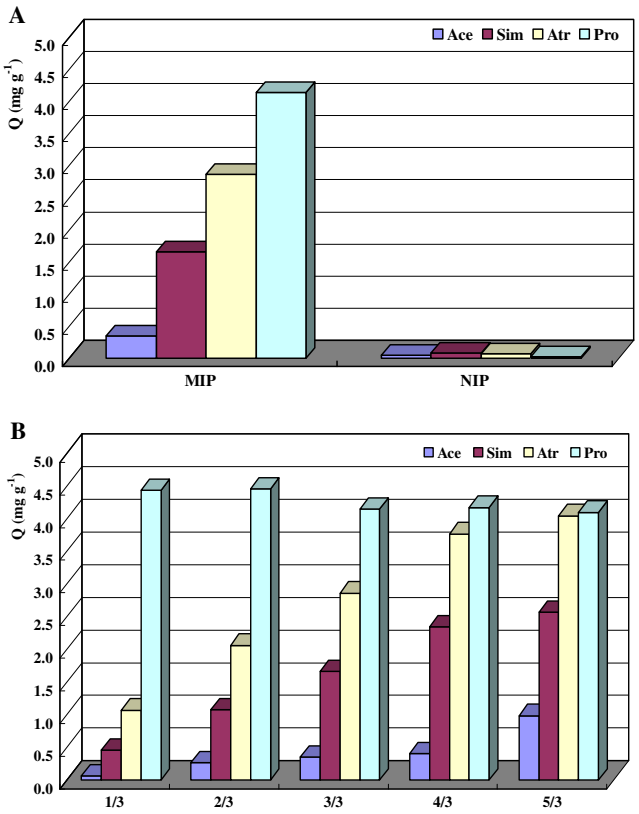

Fig. 5 Selective adsorption of Pro on MIP or NIP in mixed-solution (**A**) and in different concentration of Ace, Sim, and Atr (**B**). **A** 5 mL mixture water solutions of the four compounds (0.03 mmol L^{-1}) with 5.0 mg of MIP or NIP. Binding time, 24 h. **B** 5 mL mixture water solutions of Pro (0.03 mmol L^{-1}) and the other compounds (0.01–0.05 mmol L^{-1}) with 5.0 mg of MIP. Binding time, 24 h

amount of the analogues was much higher than that of Ace, indicating that MIP also possessed high selectivity to the structural analogues of Pro. Atr is more similar to Pro in molecular dimensions, making it have a higher binding affinity than Sim. Compared with Pro, the mismatch of the structure and size with specific cavities might hinder Ace entering the imprinted cavities and lead to the lowest binding amount of Ace among the four compounds. In contrast, there was no obvious difference of the NIP binding amounts for the four compounds, which likely depended on the same mechanism of nonspecific absorption.

We then investigated the effect of the concentrations of structural analogues and reference compound on adsorption selectivity of MIP. As the concentrations of Art, Sim, and Ace increased from 0.01 to 0.05 mmol L^{-1}, the MIP adsorption towards them increased (Fig. 5B). When the molar ratios of Art, Sim, and Ace to Pro concentrations were set at 3:3, 4:3, and 5:3, there was no obvious change in the binding amount of template Pro for MIP. This also suggested that the template molecule propazine had the highest affinity for the imprinted polymer than others.

Methodological validation and application to real samples

Determination of Pro, Atr, and Sim with HPLC was carried out as described above. The linearity of the calibration curves was obtained from analysis of 0.1–16 μmol L^{-1} of each analyte. Good linearity was achieved and all R^2 values were higher than 0.999 (ESM Table S1). The detection limits of instrument (LOD) for Pro, Atr, and Sim, defined as three times ratio of signal to noise (*S/N*), were 2.98, 2.95, and 3.00 nmol L^{-1}, respectively. The chromatogram of mixed standard samples (Pro, Atr, and Sim) obtained by MIP-SPE cartridge coupled with HPLC was shown in ESM Fig. S2.

The accuracy of the method was estimated by determining water, soil, and maize plant (including maize grain) samples spiked with mixed standard solutions (Pro, Atr, and Sim) at three different concentrations. As shown in ESM Table S2, the recoveries of Pro, Atr, and Sim with MIP-SPE as cartridges for the spiked water, soil, maize plant, and maize grain were 91.6–103.3, 78.0–99.8, 82.0–99.0, and 86.0–99.3 %, and the RSDs were 0.03–2.04, 0.12–6.42, 0.16–6.79, and 0.09–2.75 %, respectively. The LODs of Pro, Atr, and Sim in water, soil, maize plant, and maize grain were 2.95–3.00 nmol L^{-1},

Table 1 Results of determination of Sim, Atr, and Pro residues from real sample using MIP-SPE or C_{18}-SPE (n=3)

Samples	Pesticides	MIP		C_{18}	
		Average concentration (μmol/kg)	RSD (%)	Average concentration (μmol/kg)	RSD (%)
Soil	Sim	1.62	3.86	1.58	2.74
	Atr	1.29	3.00	1.25	1.43
	Pro	1.69	4.04	1.53	4.67
Root	Sim	0.2	1.06	0.16	2.70
	Atr	0.46	1.02	0.31	3.12
	Pro	0.69	1.72	0.46	2.04
Shoot	Sim	1.95	8.07	1.24	13.35
	Atr	1.56	9.23	1.08	8.37
	Pro	1.68	8.24	0.93	12.33

Table 2 Comparison of developed method with other methods in the literature for determination of triazine herbicides in food samples

Matrices	Extraction method	Detection method	Analytes	Sample amount (g/mL)	Organic solvent volume (mL)	Recovery (%)	LOD (μg kg^{-1})	Reference
Maize plant and grain	MIP-SPE	HPLC-UV	Triazine herbicides	1	60	82–99	0.9–1.2	Our work
Milk	ATPS	HPLC-UV	Triazine herbicides	5	1.5	86–120	2.1–2.8	[3]
Vegetables	ILFF-SPE	HPLC–UV	Triazine herbicides	5	1.4	79–104	1.3–2.7	[7]
Rice	Florisil SPE	HPLC MS	Triazine herbicides	10	22.5	82–99	2–14	[9]
Cereal and vegetable	PLE	HPLC NACE	Triazine herbicides	7	65	87–114	10–15	[40]

ATPS the aqueous two-phase system, *ILFF* ionic liquid foam floatation, *PLE* pressurized liquid extraction, *NACE* non-aqueous capillary electrophoresis

3.32–4.82, 5.43–7.06, and 4.12–6.00 nmol kg^{-1}, respectively. Although there were some impurities after the soil and maize samples were treated by MIP-SPE, they had the least impact on the quantification (ESM Fig. S3). The result showed that MIP-SPE column was able to pre-concentrate analytes.

Compared with MIP-SPE cartridge, low spiked recoveries of three herbicides were obtained by C_{18}-SPE cartridges coupled with HPLC, indicating that the MIP-SPE coupled with HPLC was more efficient for selective extraction and assessment of multi triazine herbicides at a trace level.

The MIP-SPE cartridges were then applied to purifying and concentrating triazine herbicides in real samples. Maize seedlings grew in soils with Pro, Atr, and Sim (each 4.35 μmol kg^{-1}) for 10 days. Maize shoot, root, and soil were harvested and immediately analyzed using MIP-SPE and C_{18}-SPE cartridges coupled with HPLC. The concentrations detected by MIP-SPE-HPLC in shoot, root, and soil were higher than those by C_{18}-SPE-HPLC (Table 1 and ESM Fig. S4). The MIP-SPE process consumed much less toxic organic solvent and saved much experimental time. It also showed better enrichment and purification efficiency for analytes. These results indicated that the MIP-SPE-HPLC was an efficient and effective method for selective extraction and can be applied to assessing the multi triazine herbicide residues in food and environment media.

The present method was further compared to the methods reported for the determination of triazine herbicides in complex matrices [3, 7, 9, 40]. It can be seen that the recoveries in the present method are comparable with the previous reports (Table 2). The LODs obtained by the present method are similar to or lower than these obtained by the reported methods. In addition, the MIP-SPE could be regenerated and reused for several cycles without loss in the average recovery of the triazine herbicides. The extraction device was cheap and the operation was simple when the present method was applied.

Conclusions

A new efficient propazine-MIP was synthesized by a surface molecular imprinting technique. The MIP structure was characterized by FT-IR, TEM, SEM, and XRD. The binding experiments demonstrated that MIP had a high affinity for its target and showed a cross-selectivity for a group of triazine herbicides. With MIP being applied as sorbent in SPE, propazine, atrazine, and simazine from environmental samples were successfully purified and concentrated. The method of MIP-SPE coupled with HPLC showed good recovery, high selectivity, and accuracy of quantitative analysis. The synthesized MIP also has the advantage in reproducibility. Thus, our study represents a practical, cheap, and environmental friendly method for analyzing the triazine herbicides at trace abundance in multi or complex environment media.

Acknowledgments The authors acknowledge the financial support of the Special Fund for Agro-scientific Research in the Public Interest from the Ministry of Agriculture of China (No. 201203022).

Conflict of interest The authors declare no on conflict of interest.

References

1. Wang YP, Sun Y, Xu B, Li XP, Jin R, Zhang HQ, Song DQ (2014) Magnetic ionic liquid-based dispersive liquid–liquid microextraction for the determination of triazine herbicides in vegetable oils by liquid chromatography. J Chromatogr A 1373:9–16
2. Gardi I, Nir S, Mishael YG (2015) Filtration of triazine herbicides by polymer-clay sorbents: coupling an experimental mechanistic approach with empirical modeling. Sci Direct 70:64–73
3. Yang X, Yu R, Zhang SH, Cao BC, Liu ZL, Lei L, Li N, Wang ZB, Zhang LY, Zhang HQ, Chen YH (2014) Aqueous two-phase extraction for determination of triazine herbicides in milk by high-performance liquid chromatography. J Chromatogr B 972:111–116
4. Zhou QX, Gao YY (2014) Combination of ionic liquid dispersive liquid-phase microextraction and high performance liquid chromatography for the determination of triazine herbicides in water samples. Chin Chem Lett 25:745–748
5. Fang R, Chen GH, Yi LX, Shao YX, Zhang L, Cai QH, Xiao J (2014) Determination of eight triazine herbicide residues in cereal and vegetable by micellar electrokinetic capillary chromatography with on-line sweeping. Food Chem 145:41–48
6. Zhang LY, Wang ZB, Li N, Yu AM, Zhang HQ (2014) Ionic liquid-based foam flotation followed by solid phase extraction to determine triazine herbicides in corn. Talanta 122:43–50
7. Zhang LY, Yu RZ, Wang ZB, Li N, Zhang HQ, Yu AM (2014) Determination of triazine herbicides in vegetables by ionic liquid

foam floatation solid phase extraction high performance liquid chromatography. J Chromatogr B 953–954:132–137
8. Cavalcante RM, Lima DM, Fernandes GM, Duaví WC (2012) Relation factor: a new strategy for quality control in the determination of pesticides in environmental aqueous matrices. Talanta 93: 212–218
9. Mou RX, Chen MX, Cao ZY, Zhu ZW (2011) Simultaneous determination of triazine herbicides in rice by high-performance liquid chromatography coupled with high resolution and high mass accuracy hybrid linear ion trap-orbitrap mass spectrometry. Anal Chim Acta 706:149–156
10. Bruzzoniti MC, Sarzanini C, Costantino G, Fungi M (2006) Determination of herbicides by solid phase extraction gas chromatography–mass spectrometry in drinking waters. Anal Chim Acta 578:241–249
11. Guo LJ, Qu JR, Miao SS, Geng HR, Yang H (2013) Development of a molecularly imprinted polymer for prometryne clean-up in the environment. J Sep Sci 36:3911–3917
12. Li SH, Luo JH, Yin GH, Xu Z, Le Y, Wu XF, Wu NC, Zhang Q (2015) Selective determination of dimethoate via fluorescence resonance energy transfer between carbon dots and a dye-doped molecularly imprinted polymer. Sensors Actuators B 206:14–21
13. Chen NN, Chen L, Cheng YX, Zhao K, Wu XH, Xian YZ (2015) Molecularly imprinted polymer grafted graphene for simultaneous electrochemical sensing of 4,4-methylene diphenylamine and aniline by differential pulse voltammetry. Talanta 132:155–161
14. Gohary NAE, Madbouly A, Nashar RME, Mizaikoff B (2015) Synthesis and application of a molecularly imprinted polymer for the voltammetric determination of famciclovir. Biosens Bioelectron 65:108–114
15. Zhang YY, Gao BJ, An FQ, Xu ZQ, Zhang TT (2014) Adsorption and recognition characteristics of surface molecularly imprinted polymethacrylic acid/silica toward genistein. J Chromatogr A 1359:26–34
16. Guo H, Yuan DY, Fu GQ (2015) Enhanced surface imprinting of lysozyme over a new kind of magnetic chitosan submicrospheres. J Colloid Interface Sci 440:53–59
17. Manzoor S, Buffon R, Rossi AV (2015) Molecularly imprinted solid phase extraction of fluconazole from pharmaceutical formulations. Talanta 134:1–7
18. Radi A, El-Naggar A, Nassef HM (2014) Molecularly imprinted polymer based electrochemical sensor for the determination of the anthelmintic drug oxfendazole. J Electroanal Chem 729:135–141
19. Ruela ALM, Figueiredo EC, Pereira GR (2014) Molecularly imprinted polymers as nicotine transdermal delivery systems. Chem Eng J 248:1–8
20. Qu JR, Zhang JJ, Gao YF, Yang H (2012) Synthesis and utilisation of molecular imprinting polymer for clean-up of propachlor in food and environmental media. Food Chem 135:1148–1156
21. Fu XW, Wu YJ, Qu JR, Yang H (2012) Preparation and utilization of molecularly imprinted polymer for chlorsulfuron extraction from water, soil, and wheat plant. Environ Monit Assess 184:4161–4170
22. Tang KJ, Gu XH, Luo QS, Chen SW, Wu LY, Xiong JH (2014) Preparation of molecularly imprinted polymer for use as SPE adsorbent for the simultaneous determination of five sulphonylurea herbicides by HPLC. Food Chem 150:106–112
23. Miao SS, Wang HZ, Lu YC, Geng HR, Yang H (2014) Preparation of Dufulin imprinted polymer on surface of silica gel and its application as solidphase extraction sorbent. Environ Sci Process Impact 16:932–941
24. Zarejousheghani M, Fiedler P, Moder M, Borsdorf H (2014) Selective mixed-bed solid phase extraction of atrazine herbicide from environmental water samples using molecularly imprinted polymer. Talanta 129:132–138
25. Tong YJ, Li HD, Guan HM, Zhao JM, Majeed S, Anjum S, Liang F, Xu GB (2013) Electrochemical cholesterol sensor based on carbon nanotube @ molecularly imprinted polymer modified ceramic carbon electrode. Biosens Bioelectron 47:553–558
26. Bueno L, El-Sharif HF, Salles MO, Boehm RD, Narayan RJ, Paixão TRLC, Reddy SM (2014) MIP-based electrochemical protein profiling. Sensors Actuators B 204:88–95
27. Li H, Li G, Li ZP, Lu CM, Li YA, Tan XZ (2013) Surface imprinting on nano-TiO_2 as sacrificial material for the preparation of hollow chlorogenic acid imprinted polymer and its recognition behavior. Appl Surf Sci 264:644–652
28. Li H, Xu MM, Wang SS, Lu CM, Li ZP (2014) Preparation, characterization and selective recognition for vanillic acid imprinted mesoporous silica polymers. Appl Surf Sci. doi:10.1016/j.apsusc.2014.12.085
29. Fan HT, Li J, Li ZC, Sun T (2012) An ion-imprinted amino-functionalized silica gel sorbent prepared by hydrothermal assisted surface imprinting technique for selective removal of cadmium(II) from aqueous solution. Appl Surf Sci 258:3815–3822
30. Pan JM, Xu LC, Dai JD, Li XX, Hang H, Huo PW, Li CX, Yan YS (2011) Magnetic molecularly imprinted polymers based on attapulgite/Fe_3O_4 particles for the selective recognition of 2,4-dichlorophenol. Chem Eng J 174:68–75
31. Silva HD, Pacheco JG, Magalhães JM, Viswanathan S, Delerue-Matos C (2014) MIP-graphene-modified glassy carbon electrode for the determination of trimethoprim. Biosens Bioelectron 52: 56–61
32. Rao W, Cai R, Yin YL, Long F, Zhang ZH (2014) Magnetic dummy molecularly imprinted polymers based on multi-walled carbon nanotubes for rapid selective solid-phase extraction of 4-nonylphenol in aqueous samples. Talanta 128:170–176
33. Xu WZ, Zhou W, Xu PP, Pan JM, Wu XY, Yan YS (2011) A molecularly imprinted polymer based on TiO_2 as a sacrificial support for selective recognition of dibenzothiophene. Chem Eng J 172:191–198
34. Lu YC, Zhang S, Yang H (2015) Acceleration of the herbicide isoproturon degradation in wheat by glycosyltransferases and salicylic acid. J Hazard Mater 283:806–814
35. Gao DM, Zhang ZP, Wu MH, Xie CG, Guan GJ, Wang DP (2007) A surface functional monomer-directing strategy for highly dense imprinting of TNT at surface of silica nanoparticles. J Am Chem Soc 129:7859–7866
36. Gholivand MB, Karimian N, Malekzadeh G (2012) Computational design and synthesis of a high selective molecularly imprinted polymer for voltammetric sensing of propazine in food samples. Talanta 89:513–520
37. Vasapollo G, Sole RD, Mergola L, Lazzoi MR, Scardino A, Scorrano S, Mele G (2011) Molecularly imprinted polymers: present and future prospective. Int J Mol Sci 12(9):5908–5945
38. Liu XL, Lv P, Yao GX, Ma CC, Tang YF, Wu YT, Huo PW, Pan JM, Shi WD, Yan YS (2014) Selective degradation of ciprofloxacin with modified NaCl/TiO_2 photocatalyst by surface molecular imprinted technology. Colloids Surf A Physicochem Eng Asp 441:420–426
39. Wang ZQ, Liu X, Li WQ, Wang HY, Li HX (2014) Enhancing the photocatalytic degradation of salicylic acid by using molecular imprinted S-doped TiO_2 under simulated solar light. Ceram Int 40:8863–8867
40. Carabias-Martínez R, Rodríguez-Gonzalo E, Miranda-Cruz E, Domínguez-Álvarez J, Hernández-Méndez J (2007) Sensitive determination of herbicides in food samples by nonaqueous CE using pressurized liquid extraction. Electrophoresis 28: 3606–3616